HHS Public Access

Author manuscript

Adv Healthc Mater. Author manuscript; available in PMC 2017 November 27.

Published in final edited form as:

Adv Healthc Mater. 2016 April 06; 5(7): 795–801. doi:10.1002/adhm.201500825.

Water-borne Endovascular Liquid Embolics Inspired By the Undersea Adhesive of Marine Sandcastle Worms

Joshua P. Jones[1,§], **Monika Sima**[1,§], **Ryan G. O'Hara**[2], and **Russell J. Stewart**[1,*]

[1]Department of Bioengineering, University of Utah, Salt Lake City, UT 84112

[2]Department of Radiology, University of Utah School of Medicine, Salt Lake City, UT 84112

Abstract

Transcatheter embolization is used to treat vascular malformations and defects, to control bleeding, and to selectively block blood supply to tissues. Liquid embolics are used for small vessel embolization that require distal penetration. Current liquid embolic agents have serious drawbacks, mostly centered around poor handling characteristics and toxicity. In this work, a water-borne *in situ* setting liquid embolic agent is described that is based on electrostatically condensed, oppositely charged polyelectrolytes—complex coacervates. At high ionic strengths, the embolic coacervates are injectable fluids that can be delivered through long narrow microcatheters. At physiological ionic strength, the embolic coacervates transition into a non-flowing solid morphology. Transcatheter embolization of rabbit renal arteries demonstrated capillary level penetration, homogeneous occlusion, and 100% devascularization of the kidney, without the embolic crossing into venous circulation. The benign water-borne composition and setting mechanism avoids many of the problems of current liquid embolics, and provides precise temporal and spatial control during endovascular embolization.

Graphical Abstract

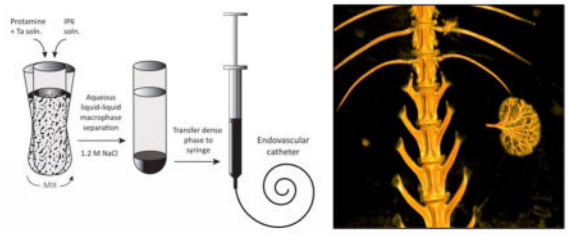

High ionic strength liquid embolic coacervates solidify when injected into renal arteries as they equilibrate to physiological ionic strength.

Introduction

The first reported transcatheter embolization was performed in 1972 to stop bleeding from a duodenal hemorrhage using an autologous clot.[1] Since then, development of embolic

*To whom correspondence should be addressed: russell.stewart@utah.edu.
§These authors contributed equally

agents has advanced significantly and clinical applications have expanded to include, among others, the occlusion of arteriovenous malformations (AVMs),[2,3] occlusion of arterial aneurysms,[4] control of gastrointestinal bleeding,[5,6] control of traumatic bleeding,[7] treatment of post-surgical varicoceles,[8] de-vascularization of head and neck tumors,[9] and chemoembolization of solid organ tumors.[10] The choice of embolic agent for a particular application is determined by the size of the vessel to be occluded, whether the occlusion is intended to be temporary or permanent, and the intended survival of the tissues supplied by the target vessel.[11] For large vessel occlusion, commonly used embolic agents include thrombosing metallic coils and plugs, plastic particles, gelatin microspheres, and gelatin foam.[11,12] Small vessels are generally occluded with liquid embolic agents that provide better distal penetration into capillaries.[13]

A major design challenge of developing liquid embolics is to provide a low viscosity formulation for delivery through long, narrow catheters and a setting mechanism for permanent occlusion at the site of delivery. The simplest liquid embolics are schlerosants—alcohols and detergents that, on contact, chemically damage the endothelial lining of the vessel, leading to localized thromboembolization.[14,15] With these agents, permanent occlusion relies on natural scarring. Another approach has been to use alkyl cyanoacrylates, low viscosity liquid resins that rapidly polymerize into hard adhesives on contact with anions present in body fluids at the delivery site. Transarterial delivery of N-butyl-2-cyanoacrylate (NBCA, TruFill®) has been approved for the treatment of cerebral AVMs since 2000. Because NBCA is adhesive and occludes blood vessels immediately and permanently, one of its drawbacks is the risk of inadvertently gluing the delivery catheter into the embolization site.[16] A third design approach has been to dissolve a water-soluble, biocompatible copolymer, ethylene vinyl alcohol (pEVOH), in a water-miscible organic solvent, dimethyl sulfoxide (DMSO), for low viscosity delivery (Onyx®, PHIL®). Upon contact with aqueous bodily fluids at the delivery site, the DMSO diffuses out and the copolymer precipitates into a solid mass to provide permanent, localized occlusion.[17] An advantage of precipitated pEVOH is that it is non-adhesive, which allows longer injection times and reduces the risk of catheter entrapment compared to NBCA. On the other hand, DMSO is toxic and can cause vasospasm, tissue necrosis, and pain if injected too rapidly, which limits the delivery rate to 0.3 mL/min, and it creates a foul taste that can persist for days.[18–20] The slow delivery rate and rapid setting makes it difficult to control forward flow and penetration with Onyx®.[21,22] Furthermore, the DMSO-borne embolics can be used only with specialized catheters that are not weakened or degraded by exposure to the organic solvent.

In this report, we describe an alternate approach to creating *in situ* setting endovascular embolic agents, an approach that originated from investigations of the undersea adhesive of sandcastle worms. The natural adhesive is packaged and stored as sets of oppositely charged polyelectrolytes (PEs) condensed into complex fluids.[23–25] Within seconds of secretion from the adhesive gland, the fluid adhesive hardens into a solid-liquid foam.[26] The transition in morphology is triggered by changes in pH, as well as ionic composition and concentrations when the fluid adhesive is exposed to seawater.[27] The *in situ* setting embolic coacervates described herein were designed to mimic the polyelectrolyte composition,

condensed fluid form, and environmentally triggered setting/hardening mechanism of the natural sandcastle glue.

In aqueous solution, sets of oppositely charged water-soluble PEs electrostatically associate and condense into several morphologies that range, depending on the solution conditions, from stable colloidal suspensions of polyelectrolyte complexes to solid precipitates or ionic hydrogels.[28] In between, within a narrow range of solution conditions, some pairs of oppositely charged PEs condense into a concentrated fluid morphology known as a complex coacervate.[29,30] Within the spectrum of morphologies in which identical compositions of PEs can exist, the phase separated fluid morphology has several ideal characteristics for use as underwater adhesives: density greater than water, relatively low viscosity for injection, low interfacial tension with water that presents a minute energetic barrier to creating new interfacial contact area on wet substrates, adhesion to wet surfaces, low water miscibility that prevents rapid dissolution into surrounding water, and dimensional stability when submerged—they do not swell by absorbing water, a severe limitation of crosslinked hydrogel-based materials.[31]

The morphology of a given set of PEs is determined by solution conditions that affect the positive to negative charge ratio and the strength of electrostatic interactions, conditions that include pH, temperature, dielectric constant, and ionic strength, which determines the degree of counterion shielding between PE charges. The morphology can be transformed along the spectrum, from fluid to solid for example, by changing solution conditions, including the concentration of monovalent counterions.[27,29] The oppositely charged PEs used in this study are phase-separated adhesive fluids—complex coacervates—at ionic strengths higher than physiological ionic strength, but insoluble adhesive gels at physiological ionic strength. When the fluid, high ionic strength adhesive coacervates are introduced into a low ionic strength environment, the fluid transitions into an adhesive gel as the ionic strength decreases. Introduced into a blood vessel through a transarterial catheter, the high ionic strength coacervates do not mix with blood, adhere strongly to the blood vessel walls, and solidify as the ionic strength decreases toward physiological ionic strength, thereby occluding the blood vessel. The embolic coacervates were tested *in vivo* by acute embolization of rabbit renal arteries.

Materials and Methods

Materials

Protamine sulfate (PRT) from salmon sperm (USP Grade), salmine, was obtained from MP Biomedical Inc. Sodium inositol hexaphosphate (IP6), also known as phytic acid, was obtained from Sigma. Tantalum metal powder, 1–5 micron particle size, was obtained from Atlantic Equipment Engineers, Inc. Sodium chloride (USP Grade) was obtained from MP Biomedical Inc. Solutions were made in ultra-pure water.

Preparation of Complex coacervates

Salmine sulfate and IP_6 were dissolved in the desired final NaCl concentration (1200 mM, unless otherwise noted) at 60 mg/mL and 115 mg/mL, pH 7.2. Ta metal powder was added

to the Sal solution to give a final concentration of 30 wt% in the condensed phase. The IP_6 and Sal/Ta solutions were mixed at a volume ratio of 1:4, resulting in a 1:1 ratio of positive to negative charges. The solution immediately turned turbid and a dense liquid macrophase (complex coacervate) settled out within an hour at 22°C. The condensed liquid phase was separated and used as the injectable *in situ* solidifying complex coacervate (Fig. 4).

Rheology

The flow behavior of Sal-IP_6 coacervates was characterized on a temperature controlled rheometer (AR 2000ex, TA Instruments) using a 20 mm, 4° cone geometry. A solvent trap prevented the sample from drying out during the experiment. Shear rate was stepped from 0.01 s^{-1} to 500 s^{-1} at 10 points per decade. Ta containing samples were run with forward and reverse shear rate sweeps. Viscosities were compared at a shear rate of 0.02 s^{-1}.

Injection pressure

For pressure measurements, 23 gauge (3F) and 18 gauge (5F) needles were glued into 1 m lengths of PTFE tubing (Zeus Inc.) of 23 and 18 gauge, respectively. Coacervates made in 1.2 M NaCl were loaded into 1 mL syringes, warmed to 37°C, and attached to the tubing. The tubing was placed in a 37°C water bath and the coacervate was injected at the specified flow rates using a syringe pump (PHD Ultra, Harvard Apparatus). To measure injection forces, a compression load cell (iLoad Mini, Loadstar Sensors) was attached to the syringe pump between the driver and the syringe plunger. Steady state injection forces were measured and converted to pressure using the bore diameter of the syringe (4.8 mm). Injection pressures were predicted using Poiseuille's equation for steady laminar fluid flow in a tube of uniform diameter:

$$\Delta P = \frac{8Q\mu L}{\pi r^4}$$

where P is pressure, r is the radius of the tube, L is the length of the tube, Q is the volumetric flow rate, and μ is viscosity.

Rabbit kidney embolization

Animal experiments were carried out under an IACUC approved protocol, following University of Utah animal research guidelines. Complex coacervates were prepared with filter-sterilized salmine sulfate and IP_6 solutions and loaded aseptically into sterile 1 mL syringes (Medallion, Merit Medical Inc.). A New Zealand white female rabbit weighing 4.5 kg was kept in an environmentally controlled animal research facility. Food was offered once a day and water was provided *ad libitum*. The rabbit was first anesthetized with Isoflurane in an induction chamber, then intubated with an endotracheal tube (3.5 mm, Hudson/Sheridan). Once intubated, the rabbit was connected to an anesthetic machine (Drager Narkomed 2B) equipped for non-invasive monitoring, including an anesthetic gas analyzer, respiratory monitor (Ohmeda 5250 RGM), oximeter, thermometer, and Isoflurane vaporizer. An intravenous infusion of 0.9% saline solution (Baxter) was administered during the procedure.

All surgical procedures were performed under sterile conditions. The inner side of the right leg was shaved, and the incision site and surrounding skin was cleaned with 70% isopropyl alcohol and covered with surgical drapes. The artery was exposed with a 5 cm longitudinal incision. The location of the incision was determined by palpating the artery. The artery was isolated from the femoral nerve and vein by blunt dissection. Two 4.0 silk sutures were positioned under the artery and used to gently elevate the artery for access. Topical Lidocaine (2%, Hospira) was administered to decrease the vasospasm of the femoral artery during handling.

The femoral artery was accessed using a 4F access kit (Access Point Technologies, Inc.). A 135 cm, 2.8F micro-catheter (Biomerics) was maneuvered from the femoral artery into the renal artery under fluoroscopy (C-arm 9800 series OEC Medical/GE medical). Omnipaque (Iohexol 240 mg/ml) was used as the X-ray contrast agent to visualize organs and blood vessels. Once the microcatether was positioned in the renal artery, Omnipaque diluted 1:1 with normal saline was injected to visualize the blood vessels of the kidney. The catheter was flushed with saline, then pre-filled with 0.2 mL of hypersaline (7.2%, 1.2 M NaCl). The coacervate containing syringe was attached to the catheter and the embolic agent was injected into the renal artery under fluoroscopic observation. The animal was euthanized with Euthanasia solution (Vet One) 90 min after the embolization procedure. Fifteen minutes post-mortem, the animal was scanned on an Axiom Artis dBA biplane angiography system (Siemens Inc.) to obtain a 3D image of the embolized kidney (Figure 5B).

Histology

During necropsy, the embolized kidney was surgically removed and fixed in 10% buffered formalin. After 2 days, the renal capsule was removed and the tissue was fixed for another 4 days. The tissue was embedded in paraffin, sectioned to 5 μm, and stained with Hematoxylin & Eosin.

Results

Formation of phase separated embolic coacervates

Polycationic salmine sulfate and polyanionic sodium inositol hexaphosphate, also known as phytic acid, were chosen as the polyelectrolytes (PEs) because both are commercially available in pharmaceutical grade. Salmine sulfate is a protamine salt purified from salmon sperm. Protamines are densely charged, strongly basic proteins that condense chromatin into the sperm head during spermatogenesis.[32] Arginine comprises 21 of the 32 amino acids of salmine (Sal).[33] Phytic acid, also known as inositol hexaphosphate (IP_6), is a natural constituent of plants, particularly as a storage form of phosphate in seeds, and an intracellular signaling molecule in animals. To determine the optimum PE ratio to maximize the yield of the condensed PE phase, Sal and IP_6 solutions in 150 mM NaCl, pH 7.2, were mixed at positive to negative charge ratios ranging from 6:1 to 1:6. Charge ratios were estimated assuming the guanidinyl sidechains of Sal were fully charged at pH 7.2 based on their 13.8 pK_a.[34] The charge density of IP_6, a weak polyanion, is strongly dependent on pH in the physiological range. IP_6 was estimated to have eight negative charges at pH 7.2 based on published acid-base titrations.[35] At high and low charge ratios the volume of condensed

phase decreased significantly. The condensed phase volume distribution was centered around the 1:1 charge ratio as expected.[30] Therefore, a charge ratio of 1:1 was used to prepare all subsequent complex coacervates.

Shrinking or swelling of the liquid form during the transition to the solid form was investigated by adding 100 μl of the liquid 1200 mM NaCl complex coacervate phase, prepared with a 1:1 charge ratio, into 1.0 ml of 150 mM NaCl. After 24 hrs, the volume of the condensed phase shrank an average of 3.0 % (n =3) during solidification.

Flow behavior vs. ionic strength

The morphology of the Sal-IP_6 compositions was adjusted from non-flowing solids to liquids by increasing the NaCl concentration, which weakened the phosphate-guanidinium charge interaction (Fig. 1). At 1200 mM NaCl, Sal-IP_6 formed clear, homogeneous, fluid complex coacervates. With decreasing NaCl, the compositions transitioned to a gel-like state, and at 150 mM NaCl were non-flowing solids. The viscosity of the compositions at 37 °C were determined as a function of ionic strength at a shear rate of 0.02 sec^{-1} (Fig. 2A). To provide x-ray contrast under a fluoroscope, 30 wt% tantalum (Ta) metal powder was added to the salmine sulfate solution before mixing with IP_6. The viscosity of the Ta-containing materials increased by more than an order of magnitude, from 1.1 to 39.7 Pa·s, going from 1200 to 150 mM NaCl. Addition of micronized Ta increased the viscosity approximately 50%, 56.8 vs. 39.7 Pa·s, in 150 mM NaCl. Flow curves for Sal-IP_6 with and without 30 wt% Ta in 1200 mM NaCl were generated by measuring the viscosity as the shear rate was swept from 0.01 to 500 sec^{-1} (Fig. 3B). Compositions containing Ta were 5–6 times more viscous than those without at very low shear rates, and displayed reversible shear thinning. Without Ta, the compositions were nearly Newtonian.

Injection Pressures

For transarterial delivery through long, narrow catheters, injection pressures must be below the burst pressure of the catheter system and within the physical limits of the operator to provide accurate control. The steady-state pressure at several flow rates in 3F and 5F catheters were compared to predicted pressures calculated from the measured viscosity of Sal-IP_6 with and without Ta in 1200 mM NaCl (Fig. 3). As expected, the injection pressure increased linearly with flow rate. The injection pressures with the 5F catheter were less than 20% higher than predicted by Pouseille's equation for steady laminar flow in a round tube. The injection pressures with the 3F catheter were up to 70% higher than predicted. At 0.5 mL per minute, the injection force was approximately 9-fold higher in the 3F model than the 5F, while predicted from the r^{-4} dependence to be 6.8-fold higher.

Rabbit Kidney Embolization

Rabbit kidneys are a convenient model for *in vivo* testing of liquid embolics for small vessel embolization.[18] The procedure for preparing the injectable embolic coacervates is diagrammed in Fig. 4. Phase separation begins immediately upon mixing sterile solutions of Sal + Ta and IP_6 in 1.2 M NaCl. The condensed Ta containing fluids were allowed to equilibrate at 22° C for 24 hrs. On the day of the procedure, 0.6 ml of the dense phase was transferred aseptically into a sterile 1 ml syringe (4.8 mm bore diameter). Vascular access to

the renal artery was gained through the femoral artery using a 0.014″ guide wire, over which a 135 cm 2.8 F microcatheter was introduced and positioned in the renal artery 1.5 cm from the first arterial branch. The catheter was pre-filled with a sterile solution of 1.2 M NaCl before the embolic containing syringe was attached to the hub of the catheter. Approximately 0.3 mL of the Sal-IP_6 embolic agent was delivered into the kidney under fluoroscopy within ~15 s, after which the catheter was withdrawn from the renal artery without applying negative pressure. No additional embolic agent left the catheter during withdrawal. No changes in breathing, or heart rate, or evidence of pain occurred during or after the injection.

The Sal-IP_6 embolic coacervate was observed by fluoroscopy to penetrate into the fine branching blood vessels of the entire renal arterial vasculature. No changes in the position or opaqueness of the embolic coacervate were observed during fluoroscopic observation for 90 min post injection (Fig. 5A). Digital subtraction angiography with an iodine contrast agent (Omnipaque) showed complete occlusion of the left kidney (Fig. S1). Post-mortem, complete and uniform embolization of the renal arteries was confirmed using in 3D reconstructions of fluorographic images (Fig. 5B, Fig. S3). Embolic agent was not observed outside of the embolization site. At the end of the experiment, the embolic coacervate was injected retrograde into the femoral artery, near the access site, before complete withdrawal of the catheter to block blood flow. The artery was fully occluded and no bleeding occurred from the access site when the catheter was withdrawn (not shown).

Histological evaluation

The embolized kidney was excised post-mortem, fixed in 10% formalin, embedded in paraffin, and sectioned for histological evaluation. Complete occlusion of arterial vessels, including arterioles, was evident throughout the renal cortex (Fig. 6A). At higher magnification, penetration of the embolic coacervate into the capillaries of the glomeruli was apparent (Fig. 6B,C). The embolic coacervate cast to the dimensions of the blood vessels with no evidence of significant *in situ* shrinking or swelling after delivery. Importantly, the embolic agent did not penetrate into the venous side of the renal cortex, or into the renal ducts (Fig. 6C, Fig. S4). Red blood cell lysis, disruption of the vascular endothelium, or adverse tissue reactions were not observed.

Discussion

The design of the *in situ* setting embolics described herein exploited both the condensed polyelectrolyte composition and environmentally triggered setting mechanism of the natural sandcastle glue. Numerous oppositely charged polyelectrolytes can be used as analogs of the natural sandcastle glue proteins to make waterborne underwater adhesives.[27,28,31] For endovascular embolic coacervates, salmine sulfate was chosen because of its long history in medical applications, including endovascular administration to reverse the anticoagulant effects of heparin.[36] Complexed with insulin (NPH insulin), salmine has been subcutaneously self-injected since 1936.[37] Likewise, IP_6 is a food additive that is generally recognized as safe (GRAS) by the FDA. Significantly, both components administered individually are quickly eliminated from blood. Salmine sulfate is eliminated from the blood

stream with a half-life of approximately 5 min.[38] IP_6 is synthesized by mammalian cells as an intracellular signaling molecule, with intracellular concentrations in the 10–50 micromolar range.[39] However, IP_6 is undetectable in normal human plasma, and when added to plasma is rapidly eliminated, likely by a plasma phosphatase.[40] The stabilities of the salmine complexed with IP_6 in the injected fluid and trapped solidified gel forms of the embolic agent are greater than the individual components, but longer term stability remains to be evaluated in future animal experiments. The rapid clearance of the individual components suggests that limited escape of the embolic components may be inconsequential.

The water-borne composition of the electrostatically condensed embolic coacervates will not require special syringes and catheters. More importantly, it eliminates the need for toxic solvents to control the viscosity and fluidity of the embolic agent. To decrease the viscosity and increase the setting time of Onyx™, additional DMSO is added to dilute the EVOH copolymer, exasperating the potentially adverse effect of the solvent. In contrast, the viscosity of the embolic coacervates can be adjusted by changing the salinity of the composition; increasing the NaCl concentrations decreases the viscosity (Fig. 2). The safety profile of endovascular injection of high concentrations of NaCl is well known. Bolus intravenous injections of hypertonic saline, some as high as 30% (5M) but most commonly 7.5% (1.28 M) are used to treat several conditions, such as increasing blood pressure after traumatic shock, with no reported adverse long-term effects.[41,42] In this study, 1.2 M NaCl (7.2%) was sufficient to achieve delivery through a 2.8 F, 135 cm microcatheter with excellent capillary penetration. Normal plasma Na^+ concentrations are 135–145 mM. Rapid injection of even several mLs of the 1.2 M NaCl embolic coacervate would have an insignificant effect of the Na^+ concentration in the ~5 L of blood in a typical adult human. Furthermore, no adverse systemic effects were observed during injection, or in the kidney tissue during histological examination (Fig. 6).

The pressure required to inject liquid embolics must not exceed the burst pressure of the catheter and must be within the physical limits of the operator. The measured pressures required for injection through the 5F catheter closely matched predictions, while the pressure in the 3F catheters were higher than predicted. At the same flow rate, the pressure in the 3F is predicted to be 6.8x higher than the 5F, whereas the measured difference was 9x higher. The discrepancy is likely due to adhesion of a thin layer of the coacervate to the catheter wall, which would have a greater effect on pressure in the narrower catheter. Nevertheless, microcatheters with rated burst pressures of 5–6 MPa are common, and the embolic coacervates were well within this pressure limit at reasonably high flow rates through both the 3F and 5F catheters. The average force that can be applied using a palmar pinch grip syringe is 23.4 lbs (104.1 N) for men and 16.3 lbs. (72.2 N) for women.[43] Using a standard 1 mL syringe, the force needed to inject the embolic coacervate through a 5F catheter at high flow rates (2 mL/min) is within the capabilities of all endovascular surgeons. The force required for the 3F catheter at high flow rates, ~20 lbs, would be challenging for some surgeons. The viscosity can be reduced by increasing the NaCl concentration. Or, the pressure exerted on the fluid can be increased by using a smaller bore syringe; reducing the bore diameter from 4.8 to 3.2 mm would decrease the force by half.

An ideal embolic agent for capillary-level occlusion would be capable of deep penetration into the capillary bed of the target tissue while providing well-controlled distal flow to prevent non-target embolism, or over-injection into the venous circulation. For pre-operative devascularization of tumors, deep tumor penetration is more effective at controlling intraoperative bleeding than simple proximal embolization.[44] Likewise, treatment of brain AVMs is more effective if the embolic fully penetrates into the nidus.[45] Although NCBA glues provide excellent penetration for these applications, they are difficult to control because the rapid polymerization requires that the injection be performed quickly and continuously once started, which diminishes precision of delivery.[44] The catheter must be drawn back immediately after injection to prevent entrapment in the blood vessel. On the other hand, distal penetration of Onyx may be limited by the slow delivery rate required to minimize DMSO vasotoxicity. Reports are mixed on the effectiveness of Onyx for deep penetration of small blood vessels.[21,44,46] Poor distal flow of Onyx can cause reflux around the catheter tip leading to non-target embolization and, in rare cases, entrapment of the catheter in the blood vessel.[47] Some surgeons deliberately create a proximal plug around the catheter tip to prevent retrograde reflux, others have combined Onyx with balloon catheters to prevent reflux. [4,22,48]

In comparison, the embolic coacervates penetrated the entire arterial vasculature of a live rabbit kidney when the delivery catheter was positioned in the main renal artery ~1.5 cm from the first primary branch (Fig. 5). The embolic entered all renal artery branches equally, and uniformly penetrated into the deepest capillaries of the renal cortex, a total distance of as much as 4 cm. Because the solidification mechanism depends on the diffusion of NaCl out of the embolic, the embolic coacervate will not harden inside the catheter. The embolic therefore can be delivered discontinuously, starting and stopping flow repeatedly with no danger of catheter entrapment. Selective embolization may be possible of multiple feeder arteries of a tumor without withdrawing the catheter. The retrograde sealing of the femoral artery after the procedure suggests that it may be possible to block several arterial feeders with a single injection from a single catheter position.[44]

Conclusions

Water-borne embolic coacervates, designed with condensed polyelectrolytes and ionic strength dependent viscosity and form, proved effective for deep distal penetration and 100% de-vascularization in acute renal embolization. The novel embolic agents have many of the flow and penetration advantages of both NCBA glues and pEVOH/DMSO liquid embolics, but few of their disadvantages. The embolic coacervates are promising agents for capillary-level occlusion of blood flow to prevent hemorrhage of vascular defects and malformations, to starve tumors, to control bleeding during tissue resection or trauma, which may extend and improve quality of human life—thanks to a reef-building worm.

Supplementary Material

Refer to Web version on PubMed Central for supplementary material.

Acknowledgments

The authors thank Dr. Lawrence McGill for help with kidney histology. The authors acknowledge they have no competing financial interests.

Funding: Funding from the Office of Naval Research (N00014-13-1-0577), the NIH (R01 HD75863), and the University of Utah, College of Engineering are gratefully acknowledged.

References

1. Rösch J, Dotter CT, Brown MJ. Radiology. 1972; 102:303. [PubMed: 4536688]
2. Linfante I, Wakhloo AK. Stroke. 2007; 38:1411. [PubMed: 17322071]
3. van Rooij WJ, Sluzewski M, Beute GN. Am J Neuroradiol. 2007; 28:172. [PubMed: 17213451]
4. Murayama Y, Viñuela F, Tateshima S, Akiba Y. Am J Neuroradiol. 2000; 21:1726. [PubMed: 11039357]
5. Loffroy R. WJGS. 2012; 4:223. [PubMed: 23467300]
6. Yap FY, Omene BO, Patel MN, Yohannan T, Minocha J, Knuttinen MG, Owens CA, Bui JT, Gaba RC. Dig Dis Sci. 2013; 58:1976. [PubMed: 23361570]
7. Lopera J. Semin intervent Radiol. 2010; 27:014.
8. Sze DY, Kao JS, Frisoli JK, McCallum SW, Kennedy WA II, Razavi MK. J Vasc Interv Radiol. 2008; 19:539. [PubMed: 18375298]
9. Lazzaro MA, Badruddin A, Zaidat OO, Darkhabani Z, Pandya DJ, Lynch JR. Front Neurol. 2011; 2:64. [PubMed: 22022319]
10. Tam KY, Leung KCF, Wang YXJ. Eur J Pharm Sci. 2011; 44:1. [PubMed: 21726636]
11. Lubarsky M, Ray CE, Funaki B. Semin Intervent Radiol. 2009; 26:352. [PubMed: 21326545]
12. Vaidya S, Tozer K, Chen J. Semin Intervent Radiol. 2008; 25:204. [PubMed: 21326511]
13. Lubarsky M, Ray C, Funaki B. Semin Intervent Radiol. 2010; 27:99. [PubMed: 21359018]
14. Duffy DM. Dermatol Surg. 2010; 36:1010. [PubMed: 20590708]
15. Do YS, Yakes WF, Shin SW, Lee BB, Kim DI, Liu WC, Shin BS, Kim DK, Choo SW, Choo IW. Radiology. 2005; 235:674. [PubMed: 15858106]
16. Pollak JS, White RI. J Vasc Interv Radiol. 2001; 12:907. [PubMed: 11487670]
17. Taki W, Yonekawa Y, Iwata H, Uno A, Yamashita K, Amemiya H. Am J Neuroradiol. 1990; 11:163. [PubMed: 2105599]
18. Wright KC, Greff RJ, Price RE. J Vasc Interv Radiol. 1999; 10:1207. [PubMed: 10527198]
19. Mottu F, Laurent A, Rufenacht DA, Doelker E. PDA J Pharm Sci Technol. 2000; 54:456. [PubMed: 11107838]
20. Guimaraes M, Wooster M. Semin intervent Radiol. 2011; 28:350. [PubMed: 22942553]
21. Blackburn SL, Kadkhodayan Y, Ray WZ, Zipfel GJ, Cross DT, Moran CJ, Derdeyn CP. J NeuroIntervent Surg. 2014; 6:536.
22. Spiotta AM, James RF, Lowe SR, Vargas J, Turk AS, Chaudry MI, Bhalla T, Janjua RM, Delaney JJ, Quintero-Wolfe S, Turner RD. J NeuroIntervent Surg. 2015; 7:721.
23. Wang, CS., Svendsen, KK., Stewart, RJ. Biological Adhesive Systems. von Beryn, J., Grunwald, I., editors. Springer-Vienna; 2010. p. 169
24. Wang CS, Stewart RJ. J Exp Biol. 2012; 215:351. [PubMed: 22189779]
25. Wang CS, Stewart RJ. Biomacromolecules. 2013; 14:1607. [PubMed: 23530959]
26. Stevens MJ, Steren RE, Hlady V, Stewart RJ. Langmuir. 2007; 23:5045. [PubMed: 17394366]
27. Shao H, Stewart R. Adv Mater. 2010; 22:729. [PubMed: 20217779]
28. Shao H, Bachus KN, Stewart RJ. Macromol Biosci. 2009; 9:464. [PubMed: 19040222]
29. Wang Q, Schlenoff JB. Macromolecules. 2014; 47:3108.
30. de Kruif CG, Weinbreck F, de Vries R. Curr Opin Colloid Interface Sci. 2004; 9:340.
31. Stewart RJ, Wang CS, Shao H. Adv Colloid Interface Sci. 2011; 167:85. [PubMed: 21081223]
32. Ansar, 2011, 1.

33. Moir RD, Dixon GH. J Mol Evol. 1988; 27:8. [PubMed: 2838640]
34. Fitch CA, Platzer G, Okon M, Garcia-Moreno BE, McIntosh LP. Protein Sci. 2015; 24:752. [PubMed: 25808204]
35. Evans WJ, McCourtney EJ, Shrager RI. J Am Oil Chem Soc. 1982; 59:189.
36. Jaques LB. Can Med Assoc J. 1973; 108:1291. [PubMed: 4122234]
37. Hagedorn HC, Jensen BN, Krarup NB, Wodstrup I. JAMA. 1936; 106:177.
38. Butterworth J, Lin YA, Prielipp RC, Bennett J, Hammon JW, James RL. Ann Thorac Surg. 2002; 74:1589. [PubMed: 12440613]
39. Letcher AJ, Schell MJ, Irvine RF. Biochem J. 2008; 416:263. [PubMed: 18684107]
40. Wilson MSC, Bulley SJ, Pisani F, Irvine RF, Saiardi A. Open Biol. 2015; 5:150014. [PubMed: 25808508]
41. Strandvik GF. Anaesthesia. 2009; 64:990. [PubMed: 19686485]
42. Järvelä K, Honkonen SE, Järvelä T, Kööbi T, Kaukinen S. Anesth Analg. 2000; 91:1461. [PubMed: 11094001]
43. Mathiowetz V, Kashman N, Volland G, Weber K, Dowe M, Rogers S. Arch Phys Med Rehabil. 1985; 66:69. [PubMed: 3970660]
44. Gore P, Theodore N, Brasiliense L, Kim LJ. Neurosurgery. 2008; 62:1204. [PubMed: 18824987]
45. Mounayer C, Hammami N, Piotin M, Spelle L, Benndorf G, Kessler I, Moret J. Am J Neuroradiol. 2007; 28:518. [PubMed: 17353327]
46. Elhammady MS, Wolfe SQ, Ashour R, Farhat H, Moftakhar R, Lieber BB, Aziz-Sultan MA. J Neurosurg. 2010; 112:1039. [PubMed: 19698039]
47. Puri AS, Rahbar R, Dearden J, Graham RJ, Lillehei C, Orbach DB. Interv Neuroradiol. 2011; 17:261. [PubMed: 21696669]
48. Gentric JC, Raymond J, Batista A, Salazkin I, Gevry G, Darsaut TE. Am J Neuroradiol. 2015; 36:977. [PubMed: 25593200]

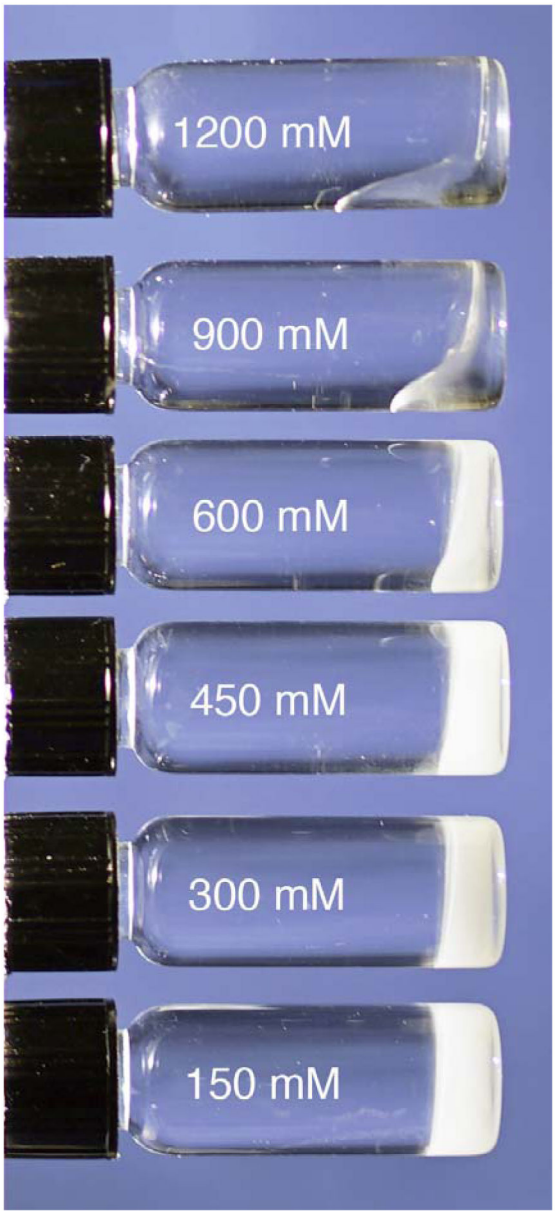

Figure 1.
Morphologies of condensed Sal-IP_6 as a function of NaCl concentration. The compositions transition from liquids at high ionic strength to stiff gels at physiological ionic strength.

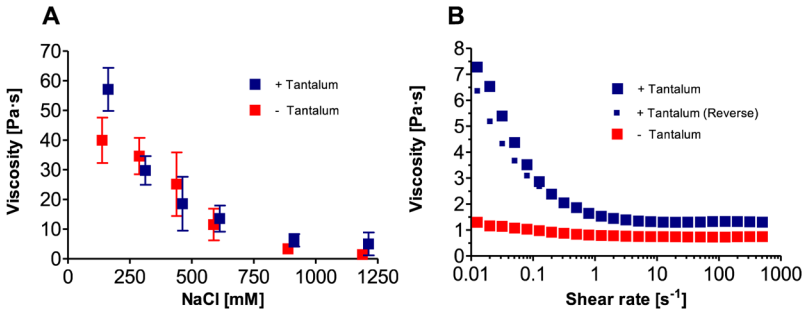

Figure 2.

Viscosity and flow behavior of Sal-IP_6. **(A)** Viscosity as a function of NaCl concentration at 37°C at a constant shear rate of 0.02 sec^{-1} (error bars represent +/− 1 s.d., n=3). **(B)** Flow curves in 1.2 M NaCl, at 37°C, with and without Ta.

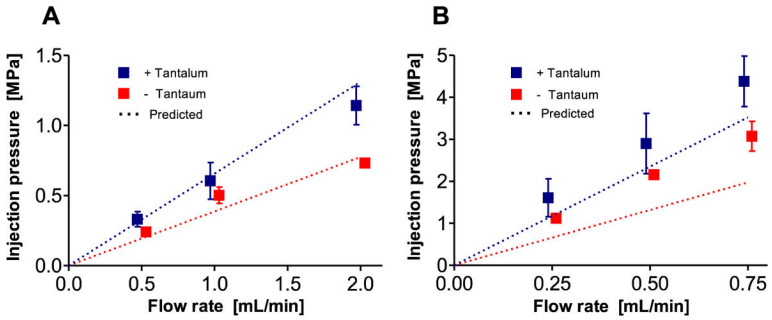

Figure 3.

Injection pressure as a function of flow rate of Sal-IP_6 in 1.2 M NaCl. A) 5F catheter. B) 3F catheter. Dashed lines are injection pressures predicted from high shear rate viscosities.

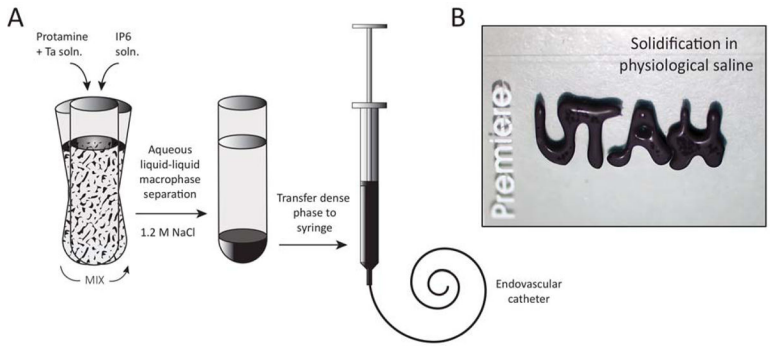

Figure 4.

A) Schematic diagram of injectable *in situ* setting Sal-IP_6 embolic coacervate preparation. The black embolic contains 30 wt% micronized Ta powder for radiopacity. B) The radiopaque, high ionic strength, low viscosity fluid rapidly solidified into a stable gel when ejected onto a 1x3 inch Premiere brand microscope slide (for scale) under physiological saline.

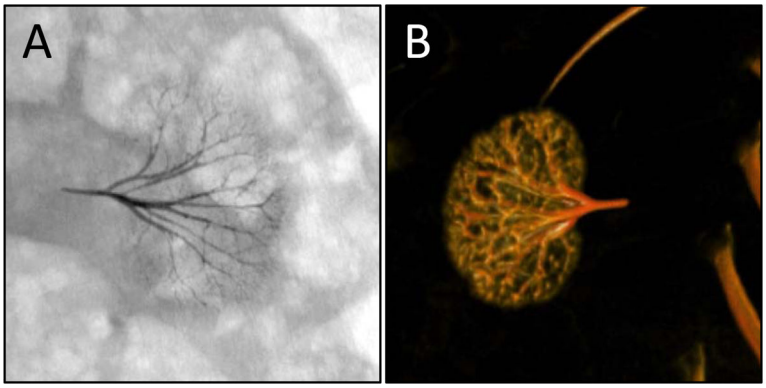

Figure 5.
Embolized rabbit kidney. (A) Ventral fluoroscope image 90 min after arterial embolization. (B) Post-mortem dorsal 3D image.

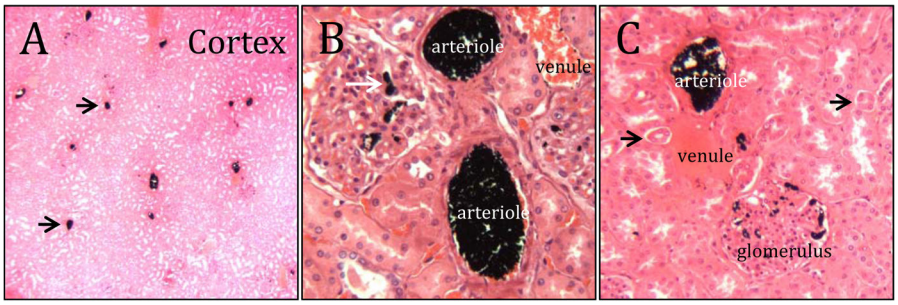

Figure 6.

Histology of embolized rabbit renal arteries. A) Low magnification cross-section through the cortex. The scattered black dots (arrows) are occluded arterioles. B) Higher magnification reveals occlusion of glomeruli capillaries (white arrow). C) The embolic coacervate was not present in venules or urine ducts (black arrows).